

# ChemComm

Accepted Manuscript



This is an *Accepted Manuscript*, which has been through the Royal Society of Chemistry peer review process and has been accepted for publication.

*Accepted Manuscripts* are published online shortly after acceptance, before technical editing, formatting and proof reading. Using this free service, authors can make their results available to the community, in citable form, before we publish the edited article. We will replace this *Accepted Manuscript* with the edited and formatted *Advance Article* as soon as it is available.

You can find more information about *Accepted Manuscripts* in the [Information for Authors](#).

Please note that technical editing may introduce minor changes to the text and/or graphics, which may alter content. The journal's standard [Terms & Conditions](#) and the [Ethical guidelines](#) still apply. In no event shall the Royal Society of Chemistry be held responsible for any errors or omissions in this *Accepted Manuscript* or any consequences arising from the use of any information it contains.

## COMMUNICATION

## On the origin of the high capacitance of nitrogen-containing carbon nanotubes in acidic and alkaline electrolytes

Cite this: DOI: 10.1039/x0xx00000x

Received 00th January 2012,  
Accepted 00th January 2012O. Ornelas,<sup>a</sup> J.M. Sieben,<sup>b</sup> R. Ruiz-Rosas,<sup>a</sup> E. Morallón,<sup>c</sup> D. Cazorla-Amoros<sup>a\*</sup>, J.Geng<sup>d\*</sup>, N. Soin<sup>d</sup> E. Siores<sup>d</sup>,  
and B. F. G. Johnson<sup>c</sup>

DOI: 10.1039/x0xx00000x

www.rsc.org/

**The synthesis of nitrogenated carbon nanotubes (N-CNTs) with up to 6.1 wt% N, via the use of pyridine as the nitrogen containing carbon precursor, can provide a facile route to significantly enhance the low intrinsic specific capacitance of carbon nanotubes. The nitrogen functionalities determine this, at least, five-fold increase of the specific capacitance.**

Carbon nanotubes (CNTs) have long been considered as a suitable material for electrochemical energy storage applications.<sup>1</sup> However, the aggregation problem caused by large van der Waals attractions, coupled with the low specific surface area and low microporosity, reduces the specific capacitance of CNTs significantly, especially when compared with other carbonaceous materials such as activated carbons and graphene. Nevertheless, the synergistic effects between the electroactive polymers such as polyaniline<sup>2</sup> and pseudocapacitive metal oxides such as RuO<sub>2</sub>, in conjunction with CNTs to enhance the specific capacitance (Cs), are well documented.<sup>3</sup>

For CNTs, a number of routes for enhancing their Cs have been explored including surface activation, enhancement of surface defect density and heteroatom doping, especially of electron donor groups such as nitrogen.<sup>4-6</sup> The heteroatom doping of nitrogen significantly alters the microstructure, electrical conductivity, chemical reactivity and electrochemical properties of CNTs including their pseudocapacitance, wherein the electrochemical behaviour itself is dependent on the dominant nitrogen moiety.<sup>4-6</sup> In general, the additional electrons provided by nitrogen are expected to produce electron donor regions.<sup>6</sup> Pyridinic and pyrrole-like functionalities are considered electroactive due to their electron donor character, whereas nitrogen atoms in imides and lactams have been proposed to be electroactive as well owing to their edge locations and the conjugation within their six-membered rings.<sup>7</sup> While all of these groups have been reported to improve the Cs of carbon materials,<sup>8</sup> the precise roles of these individual groups are poorly understood.

Here we report the exceptionally high Cs of N-doped CNTs (N-CNTs) synthesized by chemical vapour deposition (CVD) and elucidate the individual roles played by pyrrolic, pyridinic and

quaternary nitrogen groups in both acidic and basic electrolytes. The role of structural defects in enhancing the Cs is also analysed via comparison with pristine CNTs. Our one-step synthetic route provides a rapid way of enhancing the specific capacitance without the need of introducing conducting polymers or metal oxides.

The synthesis of both CNTs and N-CNTs was conducted using iron (Fe) catalyst supported on alumina ( $\gamma$ -Al<sub>2</sub>O<sub>3</sub>), with ethylene and pyridine as the respective carbon feedstock (see ESI). Thermal gravimetric analysis (TGA) of the products reveals the yield of CNTs and N-CNTs as ~30 wt% and ~10 wt%, respectively, which is consistent with the elemental analysis data (see ESI). As for producing N-CNTs, this direct CVD approach takes a clear advantage over the mostly used two-step ones where CNTs were first synthesized, then they were chemically activated and loaded with nitrogen-rich precursor to generate N-moieties on the material surface.<sup>9</sup> Moreover, the low-cost, easy-to-use of the pyridine feedstock, coupled with its structurally high ratio of nitrogen to carbon and hence the potentially highly doped nitrogen in the product, make the direct CVD route more attractive. In the two-step approaches, the surface polymer layer can be electroactive by itself<sup>10</sup> or following a decomposition by heat treatment to produce a nitrogen-rich carbonaceous deposit over the CNTs.<sup>11,12</sup> However, in the direct CVD synthesis nitrogen will be directly introduced into the carbon lattice and form structurally in-plane nitrogen groups.

Transmission electron microscopy (TEM) analysis revealed the microstructure of both pristine and N-doped carbon nanotubes produced by the direct CVD method. Both samples displayed external diameters of 20-35 nm with typical 10-12 graphene layers (Fig. 1, and also ESI). In N-CNTs, the positive curvature induced by the formation of possible N-containing pyrrolic structures resulted in faster tubular closure and the formation of multi-shell bamboo-like tubular structures.<sup>13</sup> The length, size and structure of these N-CNTs are highly mediated by the N incorporation into the graphitic lattice. Additionally, nitrogen can adopt either the sp<sup>2</sup> bonding mode (pyridinic/pyrrole functionalities) or form three C-N bonds (quaternary nitrogen). While the former functionalities are

accompanied by a C atom vacancy,<sup>14</sup> the enhanced electron transport properties could be produced by positively charged, highly coordinated nitrogen<sup>15</sup> such as quaternary nitrogen. The incorporation of nitrogen into carbon nanostructures introduces pentagonal defects in the hexagonal structure of graphene sheets, creating structural distortion and bending, leading to the graphene sheets with high curvatures, cross-linked and defective.<sup>16</sup> This increase in the defects was further confirmed by the Raman analysis (see ESI, Figure S1).

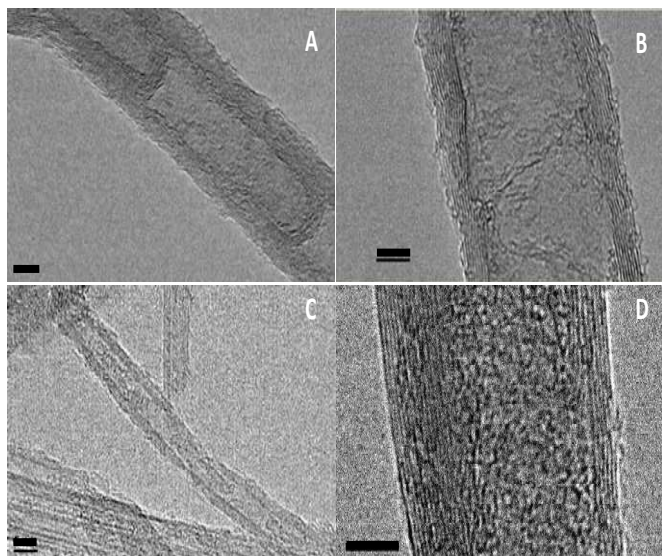


**Fig. 1** TEM images of (A,B) N-CNTs, and (C,D) CNTs produced by the direct CVD technique (bars length: 5nm).

Elemental analysis by CHN analysis and X-ray photoelectron spectroscopy revealed nitrogen content of 6.4 wt% and 6.1 wt%, respectively, with the oxygen content of N-CNTs less than 1 wt%. The core-level N1s XPS spectra was deconvoluted into three different peaks, centred at binding energies of 398.4 eV, 400.3 and 401.2 eV, respectively. They have been respectively assigned to pyridinic (N-6), pyrrolic (N-5) and quaternary nitrogen (N-Q).<sup>17</sup> Due to the low oxygen content, the presence of pyridonic groups (usually found at 400.5 eV<sup>17</sup>) would be very low, and hence the peak at 400.3 eV is assigned to pyrrolic species. The N-5 groups show the maximum contribution (48%), with the contributions from N-6 and N-Q groups being 32% and 20%, respectively.

Fig. 3 shows the cyclic voltammograms (CVs) (0-1 V vs. RHE) recorded for CNTs and N-CNTs in alkaline (6 M KOH) media at a scan rate of 50 mV·s<sup>-1</sup> (ESI Fig. S6 includes the CV in 1 M H<sub>2</sub>SO<sub>4</sub>). The characterization was done in a 3-electrode cell (see ESI for experimental details). The CVs in acidic media exhibits a quasi-rectangular-like shape for both the electrodes, while in alkaline medium the N-CNT sample shows an asymmetric-like shape. The shape observed for CNTs in both acidic and basic electrolytes indicates the absence of pseudocapacitive contribution. The slope observed in the negative sweep for N-CNTs has been attributed to the pseudocapacitive contribution of the nitrogen moieties.<sup>8</sup>

For CNT electrodes, the specific capacitances are 14 F g<sup>-1</sup> in acid medium and 21 F g<sup>-1</sup> in alkaline medium, respectively. These Cs values are in good agreement with the data for pristine MWCNTs.<sup>18</sup>

However, for the N-CNT electrodes, the Cs values are much higher at 67 and 160 F g<sup>-1</sup> in acid and alkaline medium, respectively. This huge increment observed with the N-CNTs is similar to values reported for low-porosity melamine-based nanocarbons.<sup>19</sup> Our literature search seems to suggest that there is a lack of data for the capacitance values of N-containing CNTs prepared by a similar CVD process. However, the data obtained in this work can be compared to the highest values obtained from 3-D graphene-CNT network doped with nitrogen,<sup>20</sup> and the N-doped carbon nanotubes produced by carbonization of melamine shell over a CNT core.<sup>9</sup> However, these values are lower than those of 300 F·g<sup>-1</sup> reported via the carbonization of polypyrrole over KOH-activated CNTs.<sup>10,11</sup>

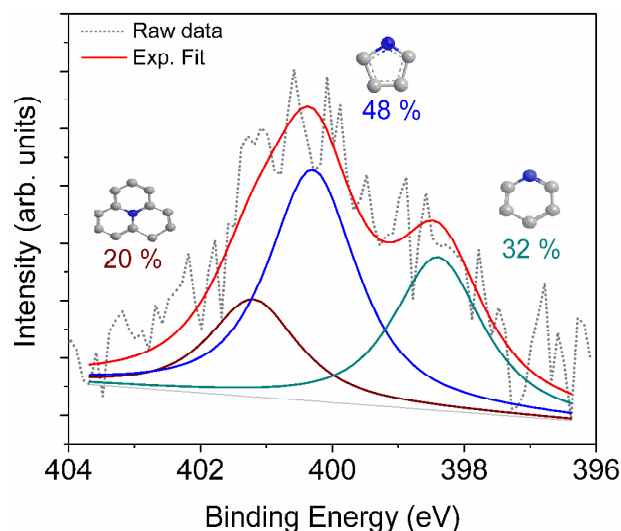


**Fig. 2** N1s core level XPS spectrum of the N-CNTs.

To elucidate how this huge enhancement of specific capacitance occurs with N-CNTs in comparison with CNTs, we investigated the contribution of each of the nitrogen moieties and the surface defects. The difference in the capacitances could arise from either (i) the ion accessibility to the nanotube surface, (ii) structural differences or (iii) pseudocapacitance and/or enhanced electron transport in N-CNTs. As for the ion accessibility to the nanotube surface, it is known that the N doping can enhance the hydrophilicity and improve the wettability of the CNT electrodes by reducing their entanglement level, since it weakens the Van der Waals forces, therefore disrupting the  $\pi$ - $\pi$  interactions and leading to weaker interactions between nanotubes<sup>14</sup>. Even so, the measured surface areal capacitance for N-CNTs is more than 75  $\mu\text{F}\cdot\text{cm}^{-2}$  (calculated from the estimated surface area obtained from the tube diameters), which is far over the expected 10-20  $\mu\text{F}\cdot\text{cm}^{-2}$  traditionally assigned to graphite-like surfaces. Thus, the capacitance enhancement in N-CNTs cannot be attributed to better ionic accessibility alone.

It is also known that the structural defects in the form of edge sites can be generated in N-CNTs via the presence of in-layer pyridine groups.<sup>21</sup> Since the double-layer capacitance of edge sites is reported to be an order of magnitude higher than that of the basal plane,<sup>22</sup> one of the contributors towards the higher capacitance of the N-CNT sample is its higher edge site to basal plane ratio, as observed in the higher Raman D/G ratio. By an estimation, we

considered that each pyridine group (as measured by XPS) can induce the formation of two C vacancies; then one can expect an additional 4% of edge sites in N-CNTs which could be responsible of a maximum of one-fold increase in the capacitance, which is clearly lower than the observed 5 to 7-fold increase. It could be argued that the structural defects could bring the internal area of the nanotubular structure more exposed to the electrolyte, like for chemically activated CNTs,<sup>23</sup> increasing the available surface area of the tubes. However, this one fold increase ascribed to the formation of higher edge sites and enhanced surface area is again not enough to explain the huge increase in the specific capacitance.

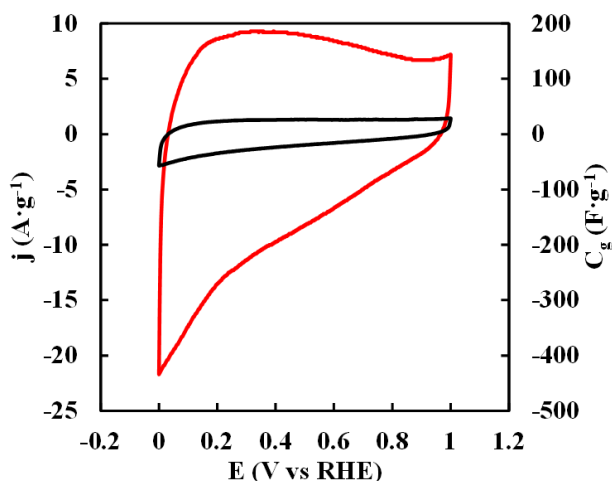


**Fig. 3** Steady-state cyclic voltammograms of N-CNT (red line) and CNT (black line) electrodes in 6 M KOH solutions at 25 °C temperature.  $v = 50 \text{ mV s}^{-1}$ . Detailed CVs measured at different scan rates can be found in ESI.

In addition to the above effects, we believe that the N-Q functional groups play a role in enhancing the capacitance. Zhu et al.<sup>24</sup> have suggested that the N-Q functionalities could be more positively charged when used as anode material in supercapacitors, attracting the negatively-charged ions more, thereby increasing the capacitance. Seredych et al. have proposed that N-Q functionalities enhance electron transport through the graphene layers.<sup>8</sup> We believe that a combination of these mechanisms could partially explain the 5-fold increment observed in acidic media, but cannot justify the very different behaviour observed in the basic media. While, the anion size is smaller for KOH than for  $\text{H}_2\text{SO}_4$  electrolyte, this difference in the ionic size is not enough to explain such a huge increment in double layer formation by enhanced ion adsorption by N-Q presence when moving from acid to basic electrolyte. Therefore, it is proposed that the N-5 and N-6 functionalities can also contribute to the capacitance through pseudocapacitance, and this contribution would be different with different electrolytes. In this regards, Moreno-Castilla et al.<sup>25</sup> have observed a good correlation between interfacial capacitance and pyrrolic and pyridinic nitrogen functionalities in acidic conditions. Thus, part of the observed capacitance enhancement of N-doped CNTs in both acidic and basic electrolytes can be attributed to the pseudocapacitance arising from the N-5 and N-6 moieties. Considering that pyrrole moieties are within the nanocaps of the bamboo-like structure of CNTs<sup>11</sup>, and are therefore inaccessible by

ions, and that Q-N does not contribute, the amount of pyridinic functionalities can be estimated to be 2.0 wt% (from XPS analyses). Assuming a one electron transfer process, the contribution of pyridinic functionalities to the capacitance is of the order of  $135 \text{ F}\cdot\text{g}^{-1}$ . This value is in good agreement with the capacitance measured in alkaline conditions ( $160 \text{ F}\cdot\text{g}^{-1}$ ), which suggests that most of the pyridinic functionalities are accessible to the electrolyte due to their location in the outer layers of the N-CNTs. The lower capacitance values for N-6 moieties in acid electrolyte can be due to their protonation in such conditions. The additional electron that may donate the N-6 moieties and the redox processes should be impeded in this medium, producing a decrease in capacitance.

## Conclusions

An efficient one-step procedure of obtaining N-containing CNTs has been developed and their electrochemical capacitance measured against pristine CNTs. For N-CNTs, a detailed assessment of various nitrogen moieties and surface defects allowed us to hypothesize the origin of the enhancement of specific capacitance, the effect of which is mainly resulting from the contribution of pseudocapacitance of redox reactions by N-6 groups, especially in basic media. On the other hand, the higher level of structural disorder and the presence of N-Q groups further enhance the formation of electrical double layer and its interaction with the anions in the electrolyte, contributing to the high capacitance. A combination of these factors provides a huge capacitance of  $160 \text{ F}\cdot\text{g}^{-1}$  in 6M KOH, bringing the possible use of these materials as flexible electrodes in micro capacitor devices.

## Acknowledgements

This work was supported by the Ministry of Economy and competitiveness of Spain (MINECO) and FEDER (MAT2010-15273, MAT2013-42007-P, CTQ2012/31762) and Generalitat Valenciana (PROMETEO/2013/038 and PROMETEOII/2014/010). OOD thanks the Generalitat Valenciana for his Grisolia grant. RRR thanks MINECO for 'Juan de la Cierva' contract (JCI-2012-12664).

## Notes and references

- Department of Inorganic Chemistry and Materials Institute, University of Alicante, Apdo. 99- 03080, Alicante, Spain. Email: cazorla@ua.es
- Inst. de Ingeniería Electroquímica y Corrosión (INIEC), Universidad Nacional del Sur, Av. Alem. 1253, Bahía Blanca (B8000CPB)- Buenos Aires – Argentina.
- Department of Physical Chemistry and Materials Institute, University of Alicante, Apdo. 99- 03080, Alicante, Spain.
- Institute for Materials Research & Innovation, University of Bolton, Deane Road, Bolton, BL3 5AB, U.K. Email: J.Geng@bolton.ac.uk
- Department of Chemistry, University of Cambridge, Lensfield Road, Cambridge, CB2 1EW, U.K.

Electronic Supplementary Information (ESI) available: synthesis of CNTs and N-CNTs, Elemental analysis, Raman spectroscopy, SEM and TEM images, Thermal gravimetric analysis, CVs recorded at different sweep rates. See DOI: 10.1039/c000000x/

- P. Simon and Y. Gogotsi, *Nat Mater*, 2008, **7**, 845–854.



2. M. Hughes, G. Z. Chen, M. S. P. Shaffer, D. J. Fray, and A. H. Windle, *Chemistry of Materials*, 2002, **14**, 1610–1613.
3. S. W. Lee, J. Kim, S. Chen, P. T. Hammond, and Y. Shao-Horn, *ACS Nano*, 2010, **4**, 3889–3896.
4. J. Ma, S. Guan, and C.-H. Lai, *Phys. Rev. B*, 2006, **74**, 205401.
5. P. Ayala, R. Arenal, M. Rummeli, A. Rubio, and T. Pichler, *Carbon*, 2010, **48**, 575–586.
6. O. Stephan, P. M. Ajayan, C. Colliex, P. Redlich, J. M. Lambert, P. Bernier, and P. Lefin, *Science*, 1994, **266**, 1683–1685.
7. M. Seredych, D. Hulicova-Jurcakova, G. Q. Lu, and T. J. Bandoz, *Carbon*, 2008, **46**, 1475–1488.
8. D. Hulicova-Jurcakova, M. Kodama, S. Shiraishi, H. Hatori, Z. H. Zhu, and G. Q. Lu, *Advanced Functional Materials*, 2009, **19**, 1800–1809.
9. K.-S. Kim and S.-J. Park, *J. Electroanal Chem*, 2012, **673**, 58–64.
10. E. Frackowiak, V. Khomenko, K. Jurewicz, K. Lota, and F. Béguin, *Journal of Power Sources*, 2006, 153, 413–418.
11. Z. Zhou, Z. Zhang, H. Peng, Y. Qin, G. Li, and K. Chen, *RSC Adv.*, 2014, 4, 5524–5530.
12. G. Lota, K. Lota, and E. Frackowiak, *Electrochem. Commun.*, 2007, **9**, 1828–1832.
13. B. G. Sumpter, V. Meunier, J. M. Romo-Herrera, E. Cruz-Silva, D. A. Cullen, H. Terrones, D. J. Smith, and M. Terrones, *ACS Nano*, 2007, **1**, 369–375.
14. R. Czerw, M. Terrones, J.-C. Charlier, X. Blase, B. Foley, R. Kamalakaran, N. Grobert, H. Terrones, D. Tekleab, P. M. Ajayan, W. Blau, M. Rühle, and D. L. Carroll, *Nano Lett.*, 2001, **1**, 457–460.
15. Z. Zhong, G. I. Lee, C. B. Mo, S. H. Hong, and J. K. Kang, *Chem. Mater.*, 2007, **19**, 2918–2920.
16. F. Villalpando-Paez, A. Zamudio, A. L. Elias, H. Son, E. B. Barros, S. G. Chou, Y. A. Kim, H. Muramatsu, T. Hayashi, J. Kong, H. Terrones, G. Dresselhaus, M. Endo, M. Terrones, and M. S. Dresselhaus, *Chemical Physics Letters*, 2006, **424**, 345–352.
17. E. Raymundo-Piñero, D. Cazorla-Amorós, A. Linares-Solano, J. Find, U. Wild, and R. Schlögl, *Carbon*, 2002, **40**, 597–608.
18. E. Frackowiak, S. Delpeux, K. Jurewicz, K. Szostak, D. Cazorla-Amorós, and F. Béguin, *Chemical Physics Letters*, 2002, 361, 35–41.
19. D. Hulicova, J. Yamashita, Y. Soneda, H. Hatori, and M. Kodama, *Chemistry of Materials*, 2005, **17**, 1241–1247.
20. B.E. Conway, *Electrochemical Capacitors: Scientific Fundamentals and Technology Applications*, 1999, New York: Kluwer.
21. M. Terrones, P. M. Ajayan, F. Banhart, X. Blase, D. L. Carroll, J. C. Charlier, R. Czerw, B. Foley, N. Grobert, R. Kamalakaran, P. Kohler-Redlich, M. Rühle, T. Seeger, and H. Terrones, *Appl Phys A*, 2002, **74**, 355–361.
22. D. Qu, *J. Power Sources*, 2002, **109**, 403–411.
23. E. Raymundo-Piñero, D. Cazorla-Amorós, A. Linares-Solano, S. Delpeux, E. Frackowiak, K. Szostak, and F. Béguin, *Carbon*, 2002, **40**, 1614–1617.
24. Z. H. Zhu, H. Hatori, S. B. Wang, and G. Q. Lu, *J. Phys. Chem. B*, 2005, **109**, 16744–16749.
25. C. Moreno-Castilla, M. B. Dawidziuk, F. Carrasco-Marín, and E. Morallón, *Carbon*, 2012, **50**, 3324–3332.